Article

Bifunctional Hybrid Mesoporous Organoaluminosilicates with Molecularly Ordered Ethylene Groups

Yongde Xia, Wenxin Wang, and Robert Mokaya

J. Am. Chem. Soc., **2005**, 127 (2), 790-798• DOI: 10.1021/ja0453230 • Publication Date (Web): 21 December 2004

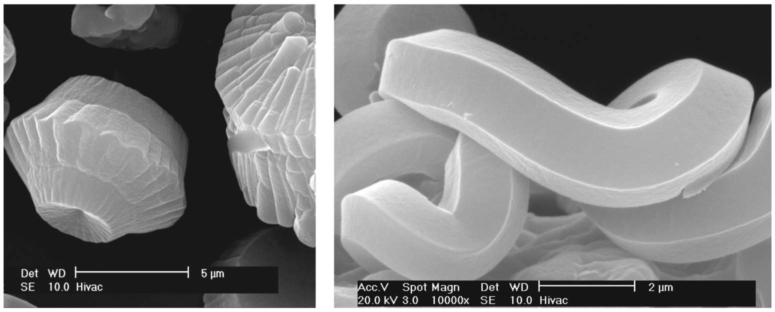

Journal of the American Chemical Society is published by the American Chemical Society. 1155 Sixteenth Street N.W., Washington, DC 20036

J|A|C|S
ARTICLES
Published on Web 12/21/2004

Bifunctional Hybrid Mesoporous Organoaluminosilicates with Molecularly Ordered Ethylene Groups

Yongde Xia, Wenxin Wang, and Robert Mokaya*

Contribution from the School of Chemistry, University of Nottingham, University Park, Nottingham NG7 2RD, U.K.

Received August 3, 2004; E-mail: r.mokaya@nottingham.ac.uk

Abstract: We report the synthesis and characterization of crystal-like structurally well-ordered ethylene-containing hybrid mesoporous organoaluminosilicate materials, which exhibit molecular-level periodicity in the pore walls and enhanced hydrothermal stability. Distilled 1,2-bis(triethoxysilyl)ethylene (BTEE) was used as the organosilica precursor, aluminum isopropoxide as aluminum source, and cetyltrimethylammonium bromide as template. The materials are structurally well-ordered and exhibit high surface area ($>$1300 m^2/g) and pore volume ($>$1.10 cm^3/g). The presence of molecularly ordered ethylene groups was confirmed by powder X-ray diffraction, ^{29}Si and ^{13}C MAS NMR, and Raman spectroscopy. The ethylene groups are thermally stable up to a temperature of 300 °C. The presence of ethylene groups enhances the hydrothermal stability in boiling water of both organosilica and organoaluminosilicate materials. The organoaluminosilicate materials possess a bifunctional character arising from the presence of both tetrahedrally coordinated Al and molecularly ordered ethylene groups in their frameworks.

Introduction

In recent years, the synthesis of silica-based mesoporous materials has been extended to organic-containing hybrid mesoporous materials via supramolecular assembly.[1,2] In particular, new synthesis strategies involving surfactant-mediated condensation of silica precursors, which have two trialkoxysilyl groups connected by an organic bridge, have attracted increasing interest since 1999.[3−6] The resulting hybrid mesoporous organosilica materials have the advantage of possessing a uniform distribution of functional organic groups both inside the pore wall (i.e., within the pore wall framework) and on the pore channel surface. The presence of organic functional groups in the mesoporous framework can tune the mechanical or optical properties of the bulk materials to produce a wide range of materials with potentially interesting electronic, magnetic, and charge-transport properties, and/or can modify the hydrophilicity/hydrophobicity of the surface and alter the surface reactivity of the materials for particular applications.[2a−c] To date, several different organic groups such as methylene,[4c] ethane,[3a,b,4f,5,6] ethylene,[4a,b,d,e,5] phenyl,[3c,d,g] bipheny,[3e] and even two- or three-substituted phenyl[3f,4g] have been incorporated into the framework of mesoporous materials. Phenyl and/or biphenyl-containing hybrid mesoporous organosilica materials were found to exhibit molecular-scale periodicity in the pore wall.[3c−g]

To date, only benzene-containing hybrid mesoporous organosilica materials have been subjected to chemical modification to generate further functionalization.[3c,7] Chemical modifications can be expected to give rise to unique physiochemical properties in the modified hybrid organosilica materials. Ethylene is a well-known active group that can be readily subjected to various chemical modifications.[4a,5,8] Previous reports on ethylene-containing mesoporous organosilicas involved either poorly ordered materials exhibiting wormhole-like pores[4a,5] or materials

---

(1) (a) Kresge, C. T.; Leonowicz, M. E.; Roth, W. J.; Vartuli, J. C.; Beck, J. S. *Nature* **1992**, *359*, 710. (b) Beck, J. S.; Vartuli, J. C.; Roth, W. J.; Leonowicz, M. E.; Kresge, C. T.; Schmitt, K. D.; Chu, C. T. W.; Olson, D. H.; Sheppard, E. W.; McCulen, S. B.; Higgins, J. B.; Schlenker, J. L. *J. Am. Chem. Soc.* **1992**, *114*, 10834.

(2) (a) Wight, A. P.; Davis, M. E. *Chem. Rev.* **2002**, *102*, 3589. (b) Stein, A.; Melde, B. J.; Schroden, R. C. *Adv. Mater.* **2000**, *12*, 1403. (c) Sayari, A.; Hamoudi, S. *Chem. Mater.* **2001**, *13*, 3151. (d) Inagaki, S. *Stud. Surf. Sci. Catal.* **2003**, *146*, 1.

(3) (a) Inagaki, S.; Guan, S.; Fukushima, Y.; Ohsuna, T.; Terasaki, O. *J. Am. Chem. Soc.* **1999**, *121*, 9611. (b) Guan, S.; Inagaki, S.; Ohsuna, T.; Terasaki, O. *J. Am. Chem. Soc.* **2000**, *122*, 5660. (c) Inagaki, S.; Guan, S.; Ohsuna, T.; Terasaki, O. *Nature* **2002**, *416*, 304. (d) Goto, Y.; Inagaki, S. *Chem. Commun.* **2002**, 2410. (e) Kapoor, M. P.; Yang, Q.; Inagaki, S. *J. Am. Chem. Soc.* **2002**, *124*, 15176. (f) Kapoor, M. P.; Yang, Q.; Inagaki, S. *Chem. Mater.* **2004**, *16*, 1209. (g) Wang, W.; Zhou, W.; Sayari, A. *Chem. Mater.* **2003**, *15*, 4886.

(4) (a) Asefa, T.; MacLachlan, M. J.; Coombs, N.; Ozin, G. A. *Nature* **1999**, *402*, 867. (b) Yoshina-Ishii, C.; Asefa, T.; Coombs, N.; MacLachlan, M. J.; Ozin, G. A. *Chem. Commun.* **1999**, 2539. (c) Asefa, T.; MacLachlan, M. J.; Grondey, H.; Coombs, N.; Ozin, G. A. *Angew. Chem., Int. Ed.* **2000**, *39*, 1808. (d) Asefa, T.; Kruk, M.; MacLachlan, M. J.; Coombs, N.; Grondey, H.; Jaroniec, M.; Ozin, G. A. *J. Am. Chem. Soc.* **2001**, *123*, 8520. (e) Dag, O.; Yoshina-Ishii, C.; Asefa, T.; MacLachlan, M. J.; Grondey, H.; Coombs, N.; Ozin, G. A. *Adv. Funct. Mater.* **2001**, *11*, 213. (f) Matos, J. R.; Kruk, M.; Mercuri, L. P.; Jaroniec, M.; Asefa, T.; Coombs, N.; Ozin, G. A.; Kamiyama, T.; Terasaki, O. *Chem. Mater.* **2002**, *14*, 1903. (g) Kuroki, M.; Asefa, T.; Whitnal, W.; Kruk, M.; Yoshina-Ishii, C.; Jaroniec, M.; Ozin, G. A. *J. Am. Chem. Soc.* **2002**, *124*, 13886.

(5) Melde, B. J.; Holland, B. T.; Blanford, C. F.; Stein, A. *Chem. Mater.* **1999**, *11*, 3302.

(6) (a) Lu, Y.; Fan, H.; Doke, N.; Loy, D. A.; Assink, R. A.; LaVan, D. A.; Brinker, C. J. *J. Am. Chem. Soc.* **2000**, *122*, 5258. (b) Sayari, A.; Hamoudi, S.; Yang, Y.; Moudrakovski, I. L.; Ripmeester, J. R. *Chem. Mater.* **2000**, *12*, 3857. (c) Hamoudi, S.; Yang, Y.; Moudrakovski, I. L.; Lang, S.; Sayari, A. *J. Phys. Chem. B* **2001**, *105*, 9118. (d) Burleigh, M. C.; Markowitz, M. A.; Wong, E. M.; Lin, J.-S.; Gaber, B. P. *Chem. Mater.* **2001**, *13*, 4411. (e) Cho, E.-B.; Kwon, K.-W.; Char, K. *Chem. Mater.* **2001**, *13*, 3837. (f) Zhu, H.; Jones, D. J.; Zajac, J.; Roziere, J.; Dutartre, R. *Chem. Commun.* **2001**, 2568. (g) Muth, O.; Schellbach, C.; Froeba, M. *Chem. Commun.* **2001**, 2032. (h) Yang, Q.; Li, Y.; Zhang, L.; Yang, J.; Liu, J.; Li, C. *J. Phys. Chem. B* **2004**, *108*, 7934.

(7) Yang, Q.; Kapoor, M. P.; Inagaki, S. *J. Am. Chem. Soc.* **2002**, *124*, 9694.

(8) Lim, M. H.; Blanford, C. F.; Stein, A. *J. Am. Chem. Soc.* **1997**, *119*, 4090.

10.1021/ja0453230 CCC: $30.25 © 2005 American Chemical Society

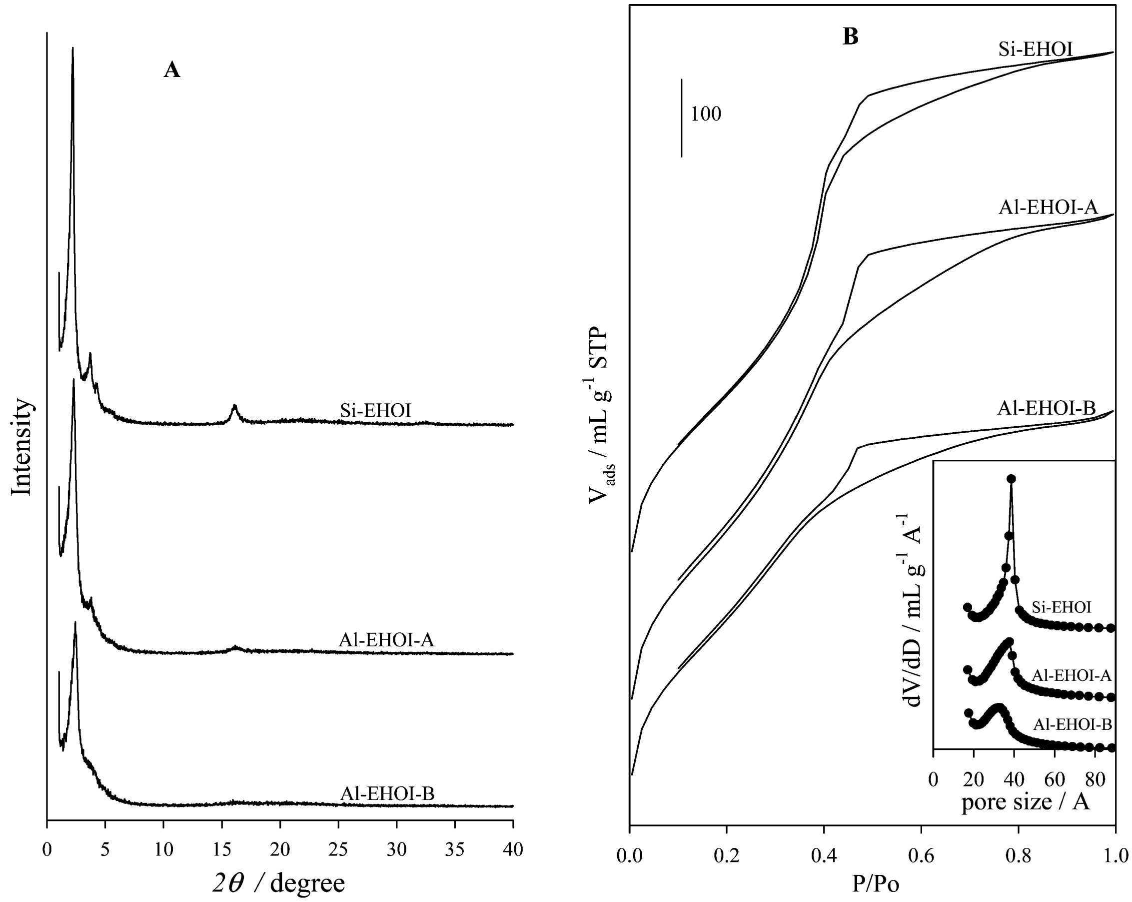

Figure 1. Powder XRD patterns (A) and nitrogen sorption isotherms (B) of surfactant-free ethylene-containing mesoporous organosilica (Si-EHOI) and organoaluminosilica (Al-EHOI) materials (see Experimental Section for sample designation). The inset in (B) shows the pore size distribution corresponding to the sorption isotherms.

with good structural ordering but without molecular-level periodicity.[9] With regard to multifunctional materials, it is desirable to synthesize ethylene-containing hybrid organosilicas which possess excellent structural ordering and molecular-scale periodicity in the pore walls. Furthermore, for applications in catalysis and separation, the incorporation of heteroatoms into the pore walls of hybrid mesoporous organosilicas offers the opportunity to introduce further functionalities (e.g., catalytic active sites). Incorporation of heteroatoms may also be used to improve other key properties, such as hydrothermal and mechanical stability, of the organosilica materials. For example, although much progress has been made on improving the hydrothermal stability of silica-based mesoporous materials,[10] the synthesis of mesoporous materials with both molecular-scale periodicity and high hydrothermal stability still remains a significant challenge. Furthermore, there are very few reports[6h,11] on the synthesis of hybrid mesoporous organoaluminosilicate materials, and these reports describe materials without molecular-scale periodicity. Herein for the first time we report the synthesis of semicrystal-like structurally well-ordered ethylene-containing hybrid mesoporous organoaluminosilicate materials, which exhibit molecular-level periodicity in the pore walls and enhanced hydrothermal stability. These materials are unique in that they possess a bifunctional character, with potentially acidic functionality associated with Al,[10] and molecularly ordered ethylene groups offering opportunity for further functionalization via simple chemical modifications.[4d,5] The materials are expected to attract interest in the fast growing field of nanostructured multifunctional materials that are ordered at various length scales.

Experimental Section

Materials Synthesis. 1,2-Bis(triethoxysilyl)ethylene (BTEE) was synthesized as previously reported.[12] Only the distilled fraction with boiling point higher than 90 °C/15 μm Hg was used. The synthesis procedure for the ethylene-containing hybrid mesoporous aluminosilicates was as follows: 4.37 g of cetyltrimethylammonium bromide (CTAB) was dissolved in 64.87 g of distilled water under stirring, followed by addition of 0.96 g of NaOH to control the pH. A quantity of 3.52 g of 1,2-bis(triethoxysilyl)ethylene was then added into the mixture, followed by the addition of a known amount of aluminum isopropoxide under stirring to give a gel mixture of molar ratio

---

(9) (a) Nakajima, K.; Lu, D.; Kondo, J. N.; Tomita, I.; Inagaki, S.; Hara, M.; Hayashi, S.; Domen, K. *Chem. Lett.* **2003**, *32*, 950. (b) Wang, W. H.; Xie, S. H.; Zhou, W. Z.; Sayari, A. *Chem. Mater.* **2004**, *16*, 1756.

(10) (a) Liu, Y.; Zhang, W.; Pinnavaia, T. J. *J. Am. Chem. Soc.* **2000**, *122*, 8791. (b) Liu, Y.; Zhang, W.; Pinnavaia, T. J. *Angew. Chem., Int. Ed.* **2001**, *40*, 1255. (c) Zhang, Z.; Han, Y.; Zhu, L.; Wang, R.; Yu, Y.; Qiu, S.; Zhao, D.; Xiao, F.-S. *Angew. Chem., Int. Ed.* **2001**, *40*, 1258. (d) On, D. T.; Kaliaguine, S. *Angew. Chem., Int. Ed.* **2001**, *40*, 3248. (e) On, D. T.; Kaliaguine, S. *Angew. Chem., Int. Ed.* **2002**, *41*, 1036. (f) Mokaya, R. *Angew. Chem., Int. Ed.* **1999**, *38*, 2930. (g) Mokaya, R. *Chem. Commun.* **2001**, 933. (h) O'Neil, A. S.; Mokaya, R.; Poliakoff, M. *J. Am. Chem. Soc.* **2002**, *124*, 10636. (i) Xia, Y.; Mokaya, R. *Microporous Mesoporous Mater.* **2004**, *68*, 1. (j) Liu, Y.; Pinnavaia, T. J. *J. Mater. Chem.* **2002**, *12*, 3179.

(11) (a) Park, S. S.; Cheon, J. H.; Park, D. H. *Stud. Surf. Sci. Catal.* **2003**, *146*, 481. (b) Kim, J.-W.; Lee, H. I.; Kim, J. M.; Yuan, X.; Yie, J. E. *Stud. Surf. Sci. Catal.* **2003**, *146*, 665.

(12) Loy, D. A.; Carpenter, J. P.; Yamanaka, S. A.; McClain, M. D.; Greaves, J.; Hobson, S.; Shea, K. J. *Chem. Mater.* **1998**, *10*, 4129.

1 BTEE:1.2 CTAB:*x* Al:2.4 NaOH:360 H_2O. After continuously being stirred for 20 h at room temperature, the synthesis gel was transferred to an autoclave and aged at 100 °C for 24 h. The autoclave was then cooled to room temperature, and the solid product was obtained by filtration and repeatedly washed with a large amount of distilled water. After air-drying at room temperature, the dry (as-synthesized) material was subjected to refluxing in an ethanol solution containing 4 wt % HCl for 2 h to extract the CTAB surfactant. The solvent extraction procedure was repeated 3 times to ensure complete removal of the surfactant. The ethylene-containing organosilica (prepared in the absence of an aluminum isopropoxide) was labeled as Si-EHOI, while organoaluminosilica samples were designated as Al-EHOI-A and Al-EHOI-B, for synthesis gel Si/Al ratio of 200 and 120, respectively. The final Si/Al ratio in the organoaluminosilica solid products was 350 for sample Al-EHOI-A and 240 for sample Al-EHOI-B. To assess hydrothermal stability, the ethylene-containing hybrid materials were refluxed in distilled water at a water-to-sample ratio of 1 L/g for various periods of time.

Table 1. Textural Properties of Surfactant-Free Ethylene-Containing Hybrid Organosilica and Organoaluminosilica Mesoporous Materials before and after Hydrothermal Treatment in Boiling Water

sample	d_{100} spacing (Å)	surface area ($m^2\ g^{-1}$)	pore volume ($cm^3\ g^{-1}$)	pore size[a] (Å)	wall thickness[b] (Å)
Si-EHOI	40.8	1296	1.26	39.0	8.1
ref 48 h	38.7	853	0.92		
ref 96 h	39.2	845	0.87		
Al-EHOI-A	39.0	1372	1.20	35.0	10.0
ref 48 h	39.2	1199	1.16		
ref 96 h	39.0	1309	1.26		
Al-EHOI-B	37.8	1366	1.09	32.0	11.6
ref 48 h	38.4	1122	1.17		
ref 96 h	38.8	1168	0.81		

[a] Average pore size calculated using BJH analysis of the nitrogen adsorption isotherm. [b] Pore wall thickness = a_o − pore size, where a_o (lattice parameter) = $2d_{100}\sqrt{3}$.

Characterization. Powder X-ray diffraction (XRD) analysis was performed using a Philips 1830 powder diffractometer with Cu Kα radiation (40 kV, 40 mA), 0.02° step size and 2-s step time. Nitrogen sorption isotherms, pore size ditsributions, and textural properties of the materials were determined at −196 °C using nitrogen in a conventional volumetric technique by a Micromeritics ASAP 2020 sorptometer. Before analysis, the samples were oven-dried at 150 °C and evacuated for 12 h at 200 °C under vacuum. The surface area was calculated using the BET method based on adsorption data in the partial pressure (P/P_0) range 0.05−0.2, and total pore volume was determined from the amount of the nitrogen adsorbed at P/P_0 = ca. 0.99. The pore

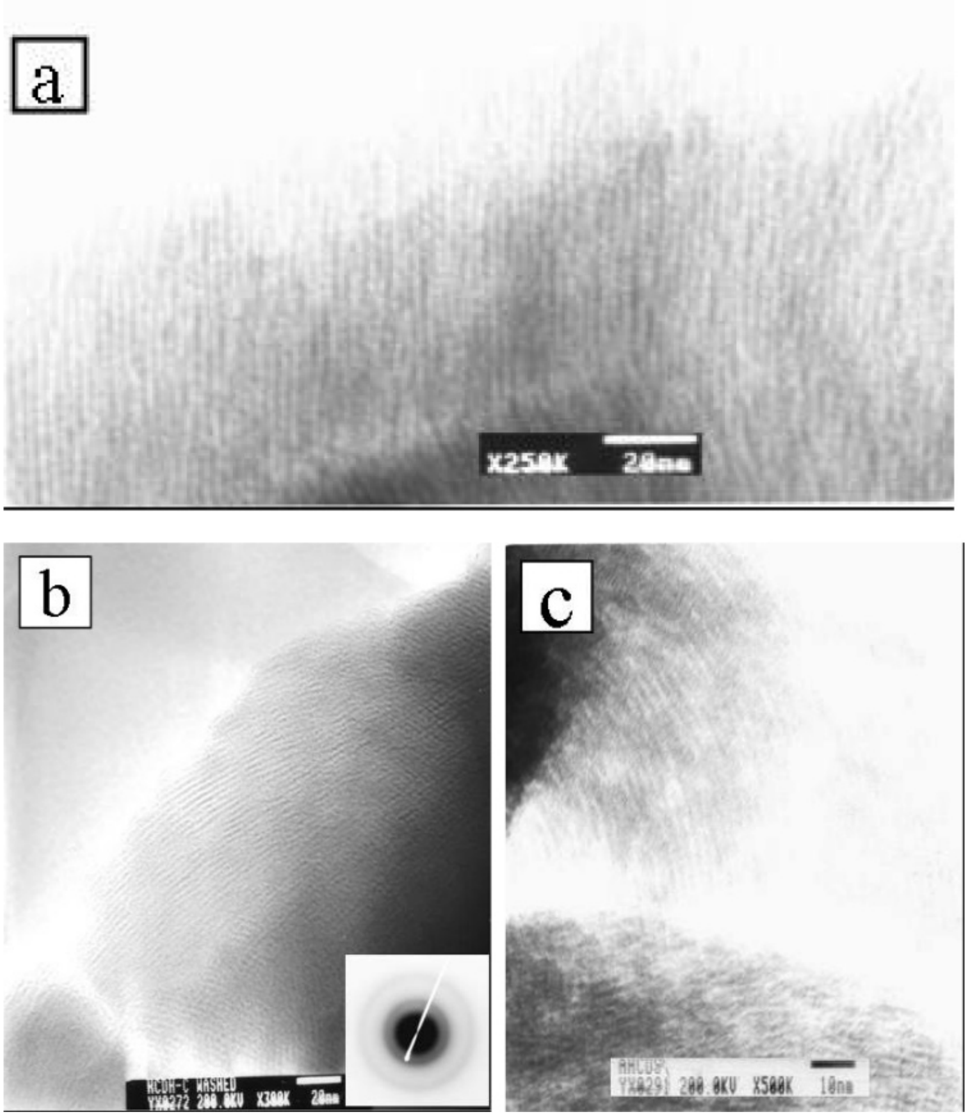

Figure 2. Representative TEM images of ethylene-containing hybrid mesoporous materials. (a, b) Organosilica, Si-EHOI, and (c) organoaluminosilica, Al-EHOI-B. The inset in (b) is the corresponding SAED pattern.

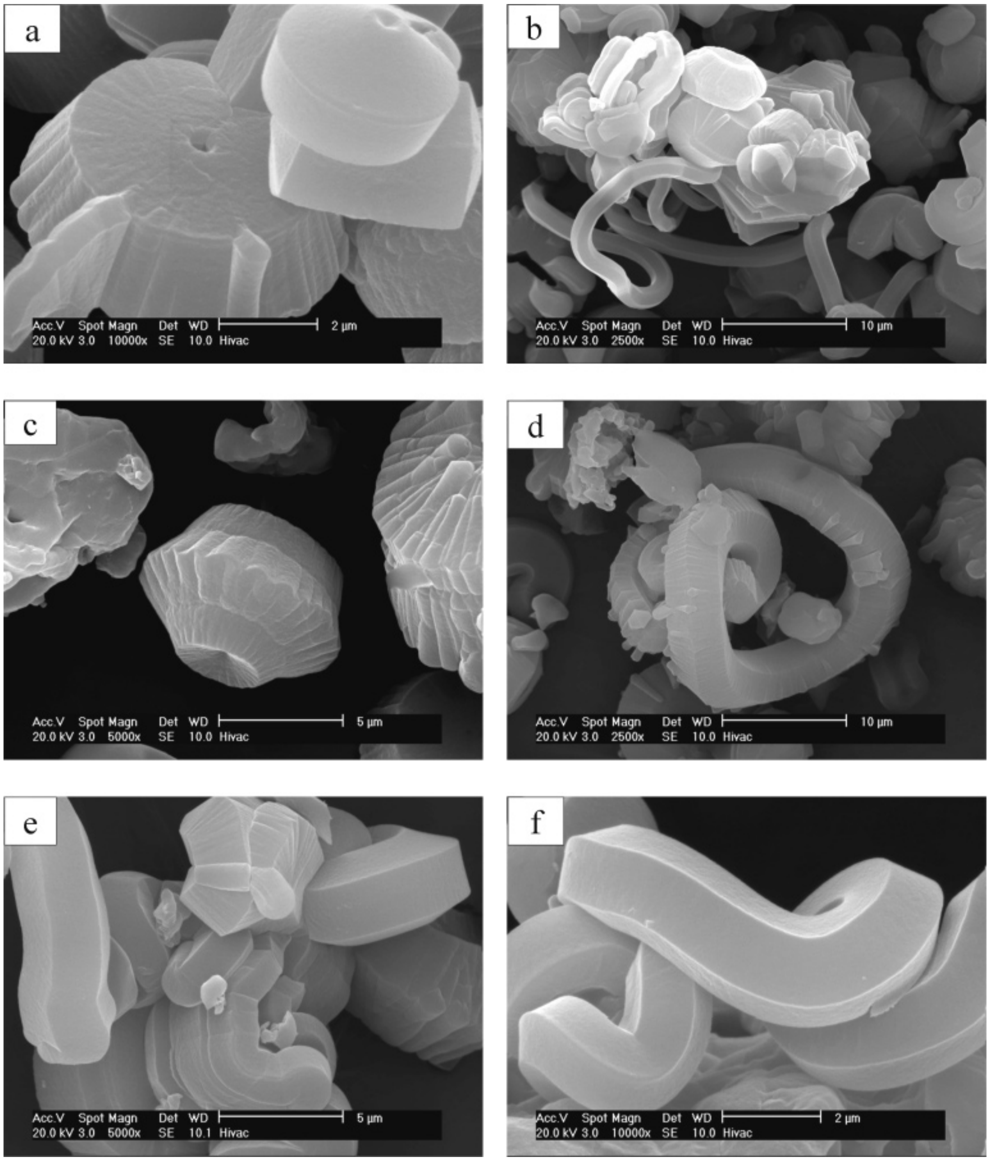

Figure 3. Representative SEM images of ethylene-containing hybrid mesoporous organosilica, Si-EHOI, (a,b) and organoaluminosilica materials with various Al content, Al-EHOI-A (c,d) and Al-EHOI-B (e,f). (See Experimental Section for sample designation.)

size distribution and average pore size were obtained from adsorption data using the BJH method. Thermogravimetric analysis (TGA) was performed using a Perkin-Elmer Pyris 6 TGA analyzer with a heating rate of 10 °C/min under static air conditions. ^{29}Si and ^{13}C magic angle spinning (MAS) nuclear magnetic resonance (NMR) spectra were acquired at room temperature using a 7.5-mm probe. ^{29}Si spectra were obtained with a ^{29}Si frequency of 59.55 MHz, spectral width of 30 kHz, 90° pulses, acquisition time of 20 ms, 120-s recycle delay, and an MAS rate of 5.1 kHz. ^{13}C spectra were obtained using a cross-polarization experiment at a frequency of 75.39 MHz, spectral width of 30 kHz with acquisition time of 30 ms, contact time of 10 ms, recycle delay of 2 s, and MAS rate of 5.0 kHz. ^{29}Si and ^{13}C signals were referenced to tetramethylsilane (TMS). ^{27}Al MAS NMR spectra were acquired at room temperature using a 4.0-mm probe at a frequency of 78.11 MHz, with an acquisition time of 5 ms, recycle delay of 0.2 s, and an MAS rate of 12.0 kHz. Raman spectra were obtained on a Nicolet Almega Dispersive Raman microscope. Raman spectra were collected by manually placing the probe tip near the desired point of the sample on a glass slide at room temperature. Transmission electron microscopy (TEM) images were recorded on a JEOL 2000-FX electron microscope operating at 200 kV. Samples for analysis were prepared by spreading them on a holey carbon film supported on a grid. Scanning electron microscopy (SEM) images were recorded using a JEOL JSM-820 scanning electron microscope. Samples were mounted using a conductive carbon double-sided sticky tape. A thin (ca. 10 nm) coating of gold sputter was deposited onto the samples to reduce the effects of charging.

Results and Discussion

Structure, Porosity, and Molecular Ordering. The structural ordering of the ethylene-containing mesoporous organosilica (designated Si-EHOI) and organoaluminosilicate (Al-EHOI) materials was assessed by powder XRD. As shown in Figure 1A, the XRD pattern for sample Si-EHOI is typical for highly ordered MCM-41 materials with an intense basal (100) diffraction peak and several well-resolved higher order peaks in the 2θ range of 3−6°. The XRD peaks can be indexed to a two-dimensional $P6mm$ hexagonal structure.[1] Remarkably, in addition to the peaks at low 2θ values, a peak at a 2θ of 16.5° is also observed. This peak is ascribed to the molecular-scale ordering of the ethylene ($-CH{=}CH-$) groups within the organosilica framework. This high-angle peak, which has not been previously reported for ethylene-containing mesoporous

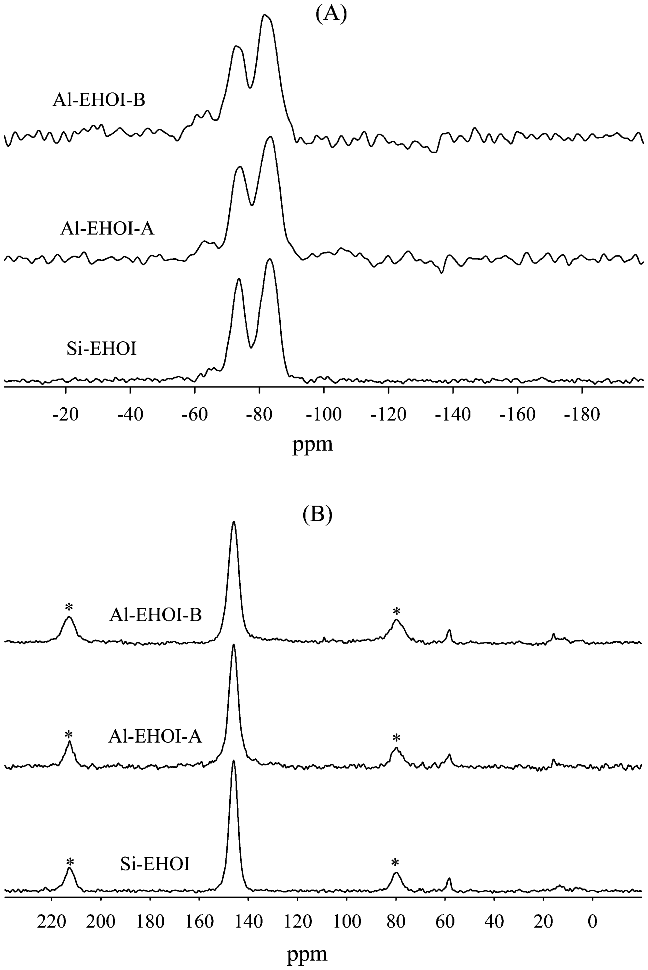

Figure 4. (A) ^{29}Si MAS NMR and (B) ^{13}C CP MAS NMR spectra of surfactant-free ethylene-containing hybrid mesoporous organosilica (Si-EHOI) and organoaluminosilica (Al-EHOI) materials. (*Denotes spinning sideband.)

organosilica materials, is assigned as a lamellar ordering of the ethylene groups with a basal spacing of 5.6 Å. In a manner similar to that of benzene-containing mesoporous organosilica materials,[3c] this high-angle peak suggests the homogeneous presence of ethylene groups with molecular-scale periodicity in the silica framework. The incorporation of Al results in a reduction in both the intensity of the (100) diffraction peak and the higher order peaks in the 2θ range of 3−6°. The XRD patterns of the organoaluminosilica hybrid materials (Figure 1A) indicate that the incorporation of Al results in a decrease in long-range structural ordering, which is similar to what has previously been observed for aluminosilicate MCM-41 materials.[13] Furthermore, the (100) peak for Al-EHOI samples is shifted to higher 2θ values, indicating a decrease in basal (d_{100}) spacing. The decrease in basal spacing is greater at higher Al content. It is worthwhile to note that the incorporation of Al also results in a decrease in the intensity of the high-angle peak associated with molecular ordering of the −CH═CH− functional groups.

The porosity and mesostructural ordering of the Si-EHOI and Al-EHOI hybrid materials were also evaluated by nitrogen sorption studies. The sorption isotherms are presented in Figure 1B, and the corresponding textural properties are summarized in Table 1. Both Si-EHOI and Al-EHOI samples exhibit type IV isotherms with a typical capillary condensation step into uniform mesopores (in the partial pressure (P/P_o) range 0.2−0.5), implying that the materials possess good mesostructural ordering. The capillary condensation step for Al-EHOI samples is shifted to slightly lower partial pressure (compared to Si-EHOI), indicating a reduction in pore size, which is consistent with the slight lattice contraction observed from the XRD patterns in Figure 1A and associated reduction in the basal (d_{100}) spacing (Table 1). The average pore size (estimated from BJH analysis of the adsorption isotherm) reduces from ca. 3.9 nm for the organosilica Si-EHOI sample to 3.5 nm (Al-EHOI-A) and 3.2 nm (Al-EHOI-B) for the organoaluminosilica materials. (We note that the absolute value of the pore size depends on the model used for calculation; however, the trend, i.e., decrease in pore size, is real.) The pore size distribution (PSD) curves of the materials (inset Figure 1B) indicate that the organosilica (Si-EHOI) sample has very narrow distribution of mesopores. The PSD curves of the organoaluminosilicas are slightly broader. However, the overall picture that emerges from the PSD curves and sorption isotherms is that all three samples possess uniform mesopores of size in the range 3.0−4.0 nm. A comparison of the pore size and basal spacing indicates that organoaluminosilica materials have thicker pore walls compared to the organosilica as reported in Table 1. Furthermore, the pore wall thickness increases at higher Al content.[13e] All the samples exhibit very high surface area (>1295 m^2/g) and pore volume (>1.0 cm^3/g). The surface area of the organoaluminosilicate samples, i.e., 1372 and 1366 m^2/g for Al-EHOI-A and Al-EHOI-B, respectively, is particularly high. The lower degree of long-range structural ordering for the organoaluminosilicate materials

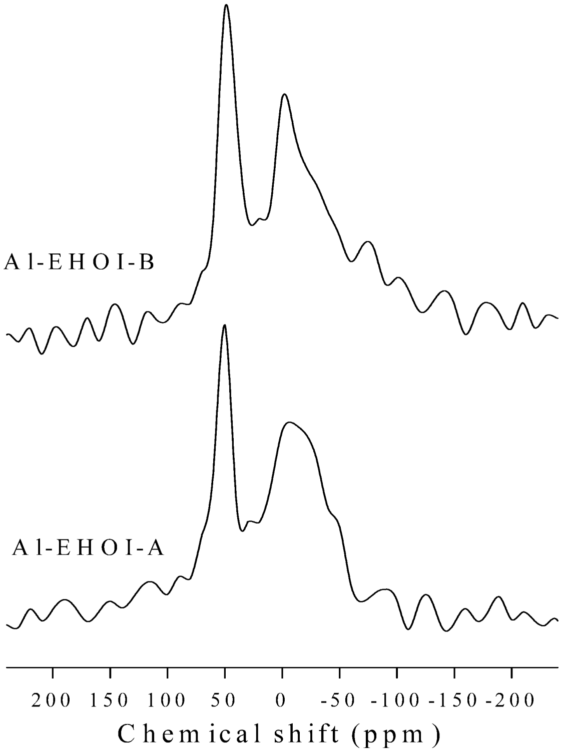

Figure 5. ^{27}Al MAS NMR spectra for surfactant-free ethylene-containing organoaluminosilica materials.

---

(13) (a) Shen, S. C.; Kawi, S. *J. Phys. Chem. B* **1999**, *103*, 8870. (b) Shen, S. C.; Kawi, S. *Langmuir* **2002**, *18*, 4720. (c) Mokaya, R. *Adv. Mater.* **2000**, *12*, 1681. (d) Mokaya, R. *J. Phys. Chem. B* **2000**, *104*, 8279. (e) Xia, Y.; Mokaya, R. *J. Phys. Chem. B* **2003**, *107*, 6954.

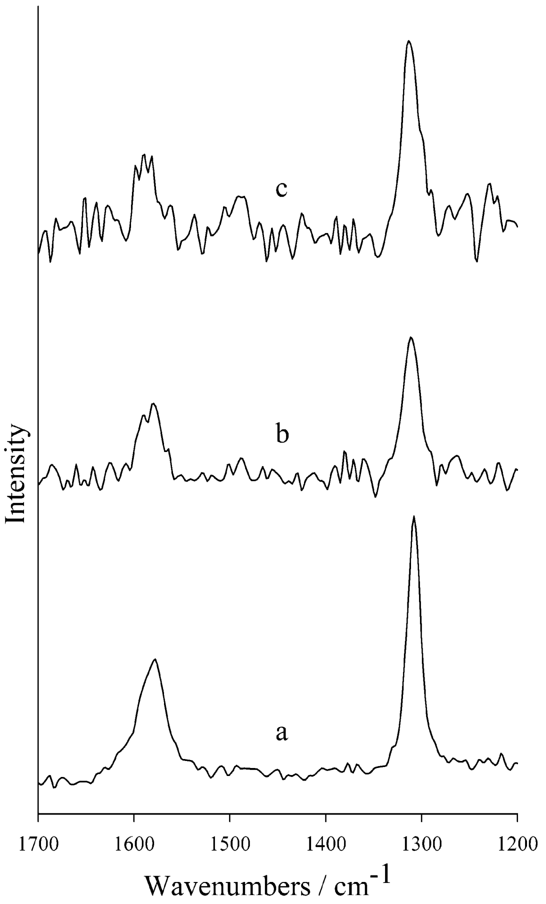

Figure 6. Raman spectra of surfactant-free organosilica, (a) Si-EHOI, and organoaluminosilicate, (b) Al-EHOI-A and (c) Al-EHOI-B, mesoporous hybrid materials with varying Al content.

(Figure 1A) does not therefore appear to have any adverse effect on their surface area and pore volume.

The structural ordering of the hybrid materials was also evidenced by TEM as shown by the representative TEM images in Figure 2. Ordered pore channels are clearly observed at the edge of the particles for both pure organosilica (Figure 2a,b) and organoaluminosilica (Figure 2c), indicating the mesostructural structural ordering of the hybrid materials. The TEM images indicate that the pore channel ordering of the organosilica (Si-EHOI) sample is better than that of the organoaluminosilicas (Al-EHOI), which is consistent with the XRD patterns of the materials (Figure 1A). The pore size obtained from the TEM images (ca. 3.5 nm) is very close to that calculated from the nitrogen sorption data. The inset in Figure 2b shows a selected area electron diffraction (SAED) pattern for the organosilica sample. The SAED pattern exhibits diffraction rings that may be ascribed to polycrystallinity arising from the presence of molecularly ordered ethylene groups within the organosilica framework. In general, such diffraction rings are not normally observed for purely siliceous mesoporous silicas. The SAED pattern therefore provides further evidence of molecular-scale periodicity in the hybrid materials.

Morphology. The particle morphology of the Si-EHOI and Al-EHOI materials was investigated by SEM. Representative SEM images are shown in Figure 3. Interestingly, both cakelike and long ropelike particles were present for the organosilica Si-EHOI sample (Figure 3a,b). The particle sizes were in the range of 3−6 μm (diameter of cakelike particles) and 30−60 μm (length of ropelike particles). The Al-EHOI-A sample (Figure 3c,d) exhibits not only cakelike particles with a diameter of 5−8 μm, but also long ropelike particles with a length of up to 60 μm. It is interesting to note that increase in the Al content (sample Al-EHOI-B) results in a particle morphology that is dominated by long ropelike particles with sharp edges; the sharp edges are consistent with the formation of long hexagonal particles as shown in Figure 3e,f. The incorporation of Al appears to have the effect of optimizing the formation of long ropelike hexagonal particles.

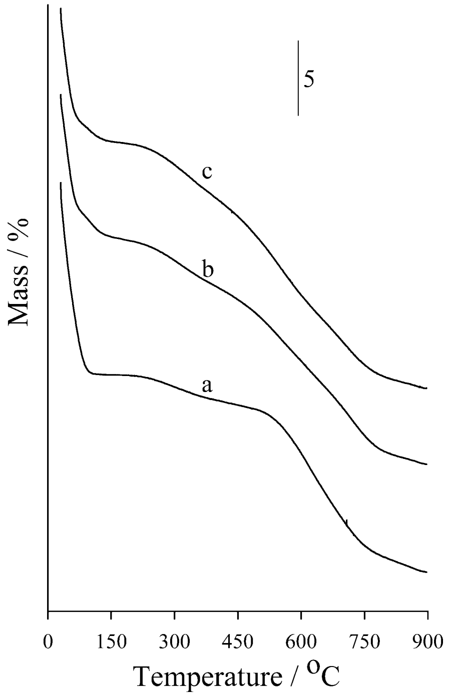

Figure 7. Thermogravimetric analysis curves of surfactant-free ethylene-containing hybrid mesoporous organosilica and organoaluminosilica materials. (a) Si-EHOI, (b) Al-EHOI-A, and (c) Al-EHOI-B.

Composition and Silica-Ethylene Bonding. Figure 4 shows the ^{29}Si and ^{13}C MAS NMR spectra obtained for the organosilica and organoaluminosilica samples. The ^{29}Si MAS NMR spectra (Figure 4A), for all three samples, exhibit two main signals at −73.7 and −83.3 ppm. The signals are assigned to silicon bonded to carbon, i.e., T^2 [C−SiO$_2$(OH)] at −73.7 ppm and T^3 [C−SiO$_3$] at −83.3 ppm. It is clear from Figure 4A that the silicon environments Q^n [(Si(OSi)$_n$(OH)$_{4-n}$), $n = 2-4$] normally observed[14] in the range −90 to −115 ppm for purely siliceous mesoporous silicas are not observed. Compared to pure silica mesophases, the ^{29}Si MAS NMR spectra of the present hybrid organosilica and organoaluminosilica materials indicate that the peaks are shifted to lower chemical shifts because of a change in the Si environment. The ^{29}Si NMR spectrum confirms that no carbon−silicon cleavage of the BTEE species occurred during synthesis of the hybrid materials. The relative intensity of the peaks suggests that a significant proportion (ca. 60%) of the Si in the hybrid materials is in T^3 (C−SiO$_3$) environment. The spectra also indicate that the organoaluminosilica materials have a higher proportion (ca. 9%) of T^1 sites (low intensity peak

---

[14] (a) Mokaya, R. *J. Phys. Chem. B* **1999**, *103*, 10204. (b) Mokaya, R.; Zhou, W.; Jones, W. *J. Mater. Chem.* **2000**, *10*, 1139. (c) Mokaya, R. *Microporous Mesoporous Mater.* **2001**, *44−45*, 119.

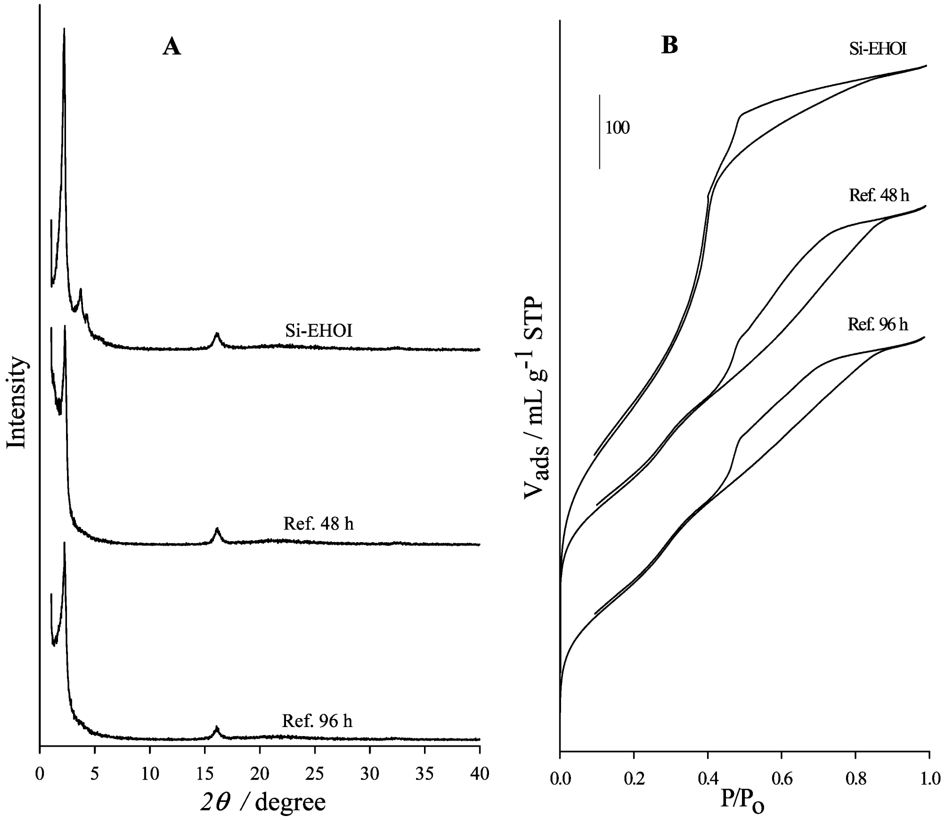

Figure 8. Powder XRD patterns (A) and nitrogen sorption isotherms (B) of ethylene-containing hybrid mesoporous organosilica before and after refluxing in boiling water for 48 or 96 h.

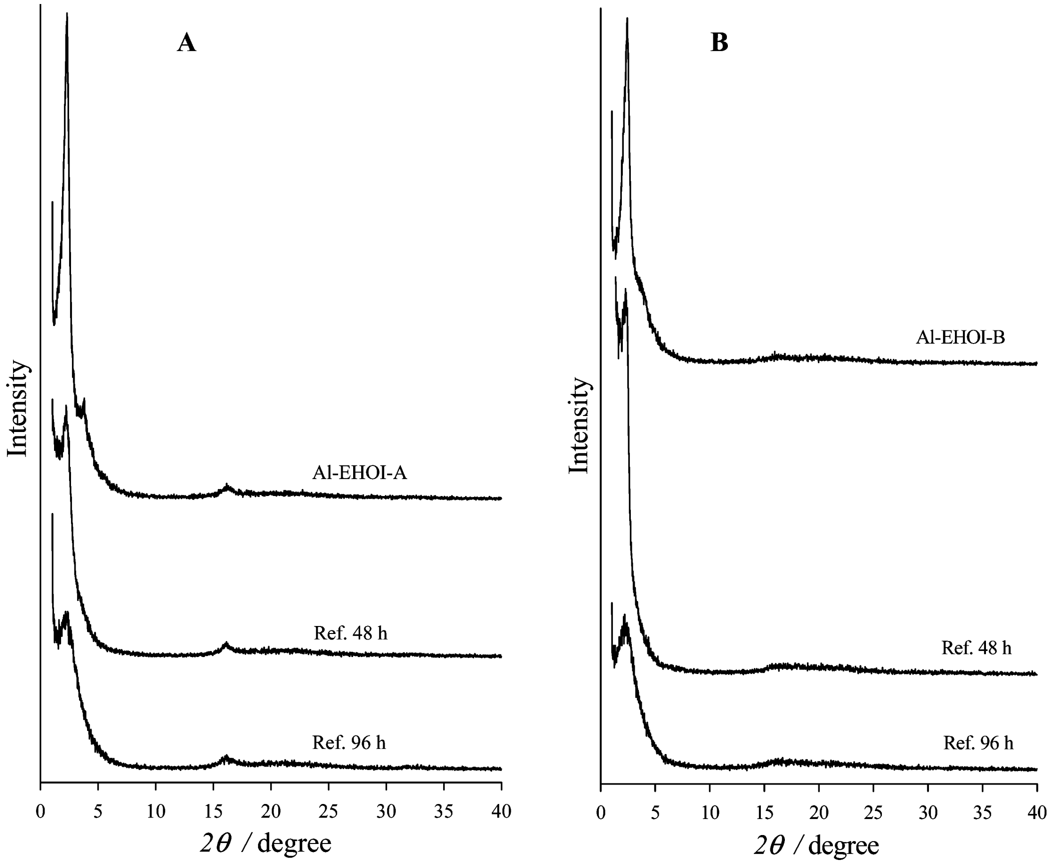

Figure 9. Powder XRD patterns of ethylene-containing hybrid mesoporous organoaluminosilicate Al-EHOI-A and Al-EHOI-B samples before and after refluxing in boiling water for 48 or 96 h.

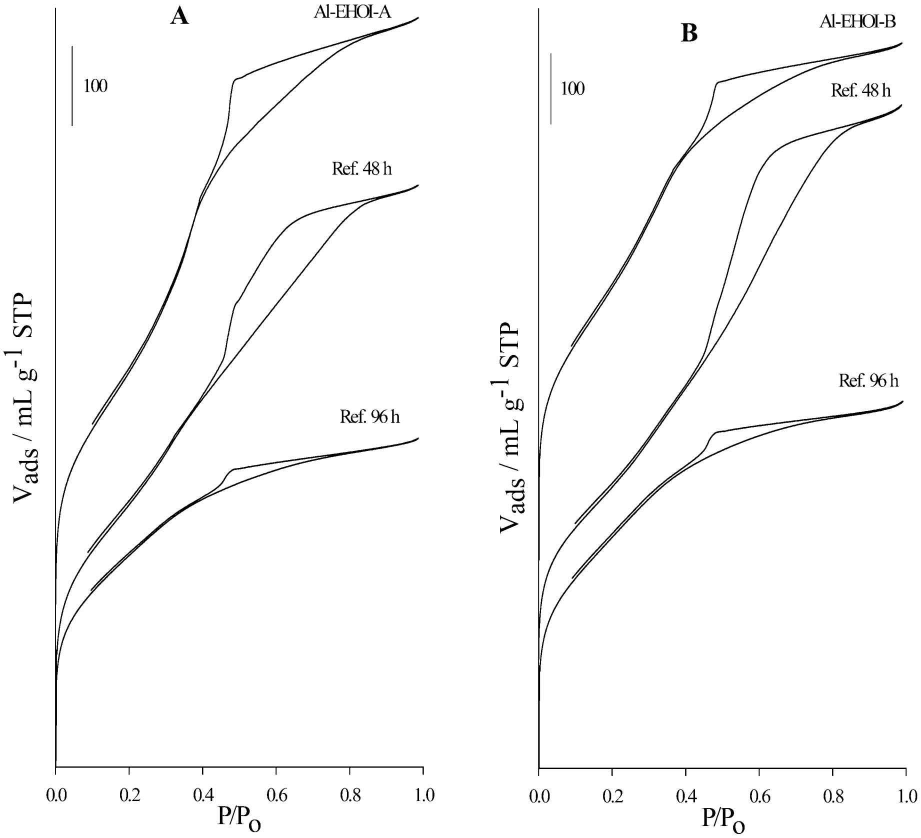

Figure 10. Nitrogen sorption isotherms of ethylene-containing hybrid mesoporous aluminosilicates before and after refluxing in boiling water for 48 or 96 h.

at ca. −64 ppm) compared to the organosilica sample (ca. 5%). The ^{13}C NMR spectra (Figure 4B) exhibit a main peak at 146 ppm due to ethylene (−CH═CH−) functional groups linked to silicon. The peaks at 58 and 18 ppm are from residual ethanol solvent.[3f] The absence of Q^n peaks in the ^{29}Si NMR spectrum suggests that hydrolysis of the silicon−ethylene bond did not occur.[3,4,9] Furthermore, the fact that the ^{13}C NMR spectrum exhibits no significant peaks in the range 10−30 ppm suggests that virtually all the CTAB surfactant was removed from the organosilica during the extraction process.[5] The NMR spectra in Figure 4 are consistent with an organosilica framework composed primarily of $(O_{1.5}Si)-CH{=}CH-SiO_{1.5}$ units.[5,9b]

Figure 5 shows the ^{27}Al MAS NMR spectra of organoaluminosilica samples. The spectra of both samples exhibit two main resonances centered at ca. 51 and 0 ppm. The resonance at 51 ppm is due to tetrahedrally coordinated Al located within the framework of the organoaluminosilica materials. This resonance indicates that Al is incorporated into the framework of the hybrid materials. The resonance at 0 ppm is due to octahedrally coordinated so-called extraframework Al. The spectra imply the presence of both framework and extraframework Al. It is noteworthy that the spectra indicate that a significant amount of the Al present in the hybrid materials is in framework tetrahedral positions. We note that the ^{27}Al MAS NMR spectra show a rather high noise/signal ratio due to the low Al content of the materials.

The existence of ethylene groups in the organosilica and organoaluminosilica frameworks was probed by Raman spectroscopy. The Raman spectra for both Si-EHOI and Al-EHOI hybrid materials, shown in Figure 6, exhibit the characteristic bands at 1578 and 1308 cm^{-1}, which correspond to the $\upsilon_{C=C}$ stretching band and the in-plane δ_{C-H} deformation of trans-bridging ethylene groups, respectively. This result is in agreement with previous reports.[4a,d,e,9] The peak intensities for Al-EHOI samples are lower than those for Si-EHOI, indicating that the incorporation of Al disrupted the framework and mesostructural ordering, which is consistent with XRD and nitrogen sorption data.

Thermal and Hydrothermal Stability. To evaluate the thermal stability of ethylene groups in the framework of the hybrid mesoporous materials, TGA was performed in air (Figure 7). The TGA curves show that, besides 8−11% weight loss below 100 °C due to desorption of physisorbed water and residual ethanol, there is a gradual decrease in weight totaling ca. 12% between 300 and 800 °C due to the decomposition of ethylene groups. The ethylene groups appear to be stable up to 300 °C as there is no significant weight loss between 100 and 300 °C. It is worth noting that both Si-EHOI and Al-EHOI samples exhibit similar weight loss in the range of 300−800 °C, implying that a comparable amount of ethylene groups is incorporated in the various samples.

We also investigated the hydrothermal stability of surfactant-free ethylene-containing hybrid mesoporous materials. Hydrothermal stability is an important factor with respect to further postsynthesis modification and application of the hybrid materials.[10,11,13−15] The presence of hydrophobic ethylene groups within the framework and on the surface was expected to enhance the hydrothermal stability. The hydrothermal stability was assessed by exposure of the materials to boiling water for various periods of time. Figure 8A shows that, after refluxing in boiling water for 96 h, the XRD pattern of sample Si-EHOI still exhibited the (100) diffraction peak, implying the retention of mesostructural ordering. This is remarkable considering that pure silica MCM-41 materials are completely destroyed after exposure to boiling water for much shorter periods of time.[13a,c,d] The enhanced hydrothermal stability for the organosilica sample, (Si-EHOI), may be ascribed to the hydophobicity introduced by the ethylene groups.[6h,15] It is remarkable that the high-angle diffraction peak at 2θ of 16.5, due to molecular ordering of ethylene groups, survived the 4 days of refluxing, indicating that exposure to hydrothermal conditions has little effect on the arrangement of the ethylene groups. Nitrogen sorption isotherms of refluxed Si-EHOI samples (Figure 8B) still exhibit type IV isotherms although the mesopore filling steps are shifted to low P/P_o values. As shown in Table 1, refluxed Si-EHOI retains 65% of its initial surface area and about 70% of pore volume.

The hydrothermal stability of the ethylene-containing organoaluminosilica materials was also investigated. As shown in Figure 9, after refluxing in boiling water for up to 96 h, the XRD patterns for the organoaluminosilica hybrid materials suggest the retention of mesostructural ordering. Molecular ordering of the ethylene groups in the organoaluminosilica samples (peak at $2\theta = 16.5°$) is not affected by the exposure to boiling water. Nitrogen sorption isotherms (Figure 10) further confirm that ethylene-containing organoaluminosilicate hybrid materials possess excellent hydrothermal stability. After exposure to boiling water (refluxing) for up to 96 h, the materials retain at least 82 and 75% of their initial surface area and pore volume, respectively. The retention of textural properties, after refluxing in boiling water, is higher for the organoaluminosilica samples (>75%) than for the organosilica material (65−70%). The presence of Al is therefore beneficial with respect to hydrothermal stability.[6h,13] We believe that hybrid organosilica and organoaluminosilica materials with other hydrophobic organic groups (such as ethane and phenyl) will have improved hydrothermal stability comparable to that observed here for ethylene-containing materials. However, the present materials are interesting because of the molecular-scale ordering of the ethylene organofunctional groups.[2,9]

Conclusions

In summary, ethylene-containing aluminosilicate hybrid mesoporous materials were successfully synthesized via surfactant-mediated assembly of distilled 1,2-bis(triethoxysilyl)ethylene (BTEE) and Al in a one-pot process. The resulting materials exhibit molecular-level periodicity (due to ethylene groups) in the pore wall and possess improved hydrothermal stability. The organoaluminosilicas are bifunctional materials, with tetrahedrally coordinated Al as a potential source of acidic functional groups and the hydrophobic ethylene groups providing a second organo functionality. The ease with which the ethylene groups may be functionalized provides a route to further chemical modification. The flexibility of the materials presented here offers new opportunities for the use of mesostructured materials as multifunctional catalysts and sorbents.

Acknowledgment. We are grateful to the EPSRC for financial support.

JA0453230

---

(15) Burleigh, M. C.; Markowitz, M. A.; Jayasundera, S.; Spector, M. S.; Thomas, C. W.; Gaber, B. P. *J. Phys. Chem. B* **2003**, *107*, 12628.